Report on benchmark results of the Alaska Landslide Tsunami Model

Prepared by: Dmitry Nicolsky

1. Introduction

Tsunamis caused by underwater slope failures constitute a significant hazard in the fjords of coastal Alaska. Kulikov *et al.,* (1998) analyzed tsunami catalog data for the Southeast Alaska and British Columbia and showed that this region has a long record of tsunami waves generated by submarine and subaerial landslides, avalanches, and rockfalls. In the majority of cases, tectonic tsunamis arriving in bays and fjords from the open ocean had wave heights smaller than those of local landslide-generated tsunamis. For example, the 1964 landslide-generated tsunami in Port Valdez devastated the waterfront and caused the 52 m (~170 ft) run-up near Shoup Bay, while the tectonic tsunami was not even noticed until a high tide late in the evening (Coulter & Migliaccio, 1966; Wilson & Tørum, 1968).

NTHMP-funded efforts in Alaska are focused on improvement of the emergency response to tsunami threat in coastal communities. To help mitigate the tsunami hazards, we subject our tsunami model, used at the Geophysical Institute, University of Alaska Fairbanks, to a series of benchmark problems proposed at the 2017 NTHMP Tsunamigenic Landslide Model Benchmarking Workshop in Galveston, Texas.

The benchmark problems deal with validating and verifying the ability of the model to accurately simulate a tsunami caused by failing of unconsolidated materials. In this report, we provide a brief description of the tsunami models used to predict a potential inundation.

2. Model of landslide-generated tsunami

The numerical model that simulates water dynamics by solving nonlinear shallow water equations:

$$\frac{\partial}{\partial t}\eta + \nabla\cdot(\eta\,\mathbf{u}) = 0, \qquad (1)$$

$$\frac{\partial}{\partial t}(\eta\,\mathbf{u}) + \nabla\cdot(\eta\,\mathbf{uu}) + g\eta\nabla\xi + \eta\boldsymbol{\tau} = 0, \qquad (2)$$

where η is the water depth, $\mathbf{u}$ is the horizontal water velocity, $\xi = h + \eta + s$ is the water level, h is the bathymetry, s is the submarine slide thickness, and the constant g is the acceleration of gravity. The runup algorithm has been described and tested through a set of the analytical, laboratory and field benchmark problems by Nicolsky *et al.*, (2011). This model, commonly used to predict propagation of long waves in the ocean and inundation of coastal areas (Synolakis & Bernard, 2006).

The system of equations (1) and (2) is supplemented with equations:

$$\frac{\partial \boldsymbol{U}}{\partial t} - \frac{1}{5}\frac{\boldsymbol{U}}{s}\frac{\partial s}{\partial t} + \frac{4}{5}(\boldsymbol{U}\cdot\nabla)\boldsymbol{U} + \frac{3}{2}g\nabla(s+h) + \frac{3}{2}g\frac{\rho_w}{\rho_s}\nabla\eta + \frac{3\mu_s}{\rho_s}\frac{\boldsymbol{U}}{s^2} = 0 \qquad (3)$$

$$\frac{\partial s}{\partial t} + \frac{2}{3}\nabla\cdot(s\boldsymbol{U}) = 0 \qquad (4)$$

to simulate propagation of the viscous depth-averaged underwater slide according to the model initially proposed by Jiang & LeBlond (1992), improved by Fine *et al.* (1998). Here, the quantity U stands for the slide velocity and μ_s is the slide viscosity.

The system of equations (1-4) was successfully used it to model landslide-generated tsunami in Seward (Suleimani *et al.*, 2011), Whittier and Valdez (Nicolsky *et al.*, 2011b; 2013). The Fine model's assumptions and applicability to simulating underwater mudflows are discussed by Jiang & LeBlond (1992, 1994) in their formulation of the viscous slide model. The model uses long-wave approximation for water waves and the deforming slide, which means that the wavelength is much greater than the local water depth, and the slide thickness is much smaller than the characteristic length of the slide along the slope (Jiang & LeBlond, 1994).

In this report, we investigate accuracy of the above coupled model to simulate landslide-generated waves. We also would like to note that the shallow water wave equations (1-2) were only utilized in the Alaska tsunami inundation modeling project until 2012. Currently, the water dynamics is modeled by a 3-D non-hydrostatic wave model (Ma *et al.,* 2012).

3. Benchmark results

Problem #2: Three-dimensional submarine solid block

This benchmark problem is based on the 3D laboratory experiments of Enet & Grilli (2007). A Gaussian -shaped solid body slides from its initial position down a plane slope built in the tank (http://www1.udel.edu/kirby/landslide/problems/benchmark_2.html). Measured data included: surface elevation at up to four capacitance wave gages 1 to 4, and the wave runup R_u on the slope. To compute the water level, we discretized the study area with $\Delta x=\Delta y=0.01$-m grid cells, the time step $\Delta t=2\cdot10^{-4}$ seconds.

Comparisons between the measured and computed water level dynamics for the initial depth of submergence d=61 mm and d=120 mm are shown in figure 1a and 1b, respectively.

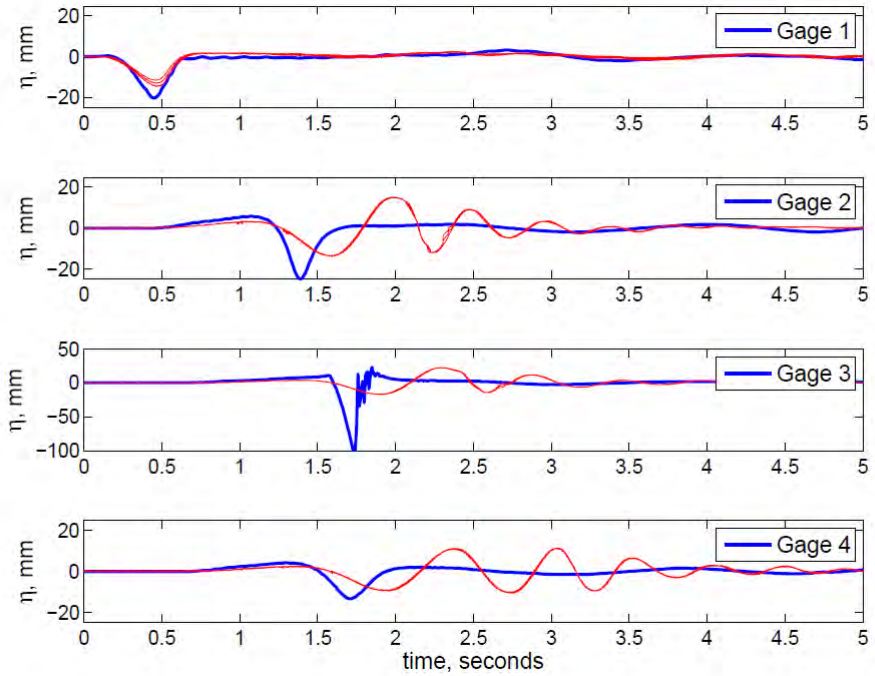

Figure 1a: Comparison of modeled (blue) and computed (red) water level dynamics for the initial submergence d=61 mm.

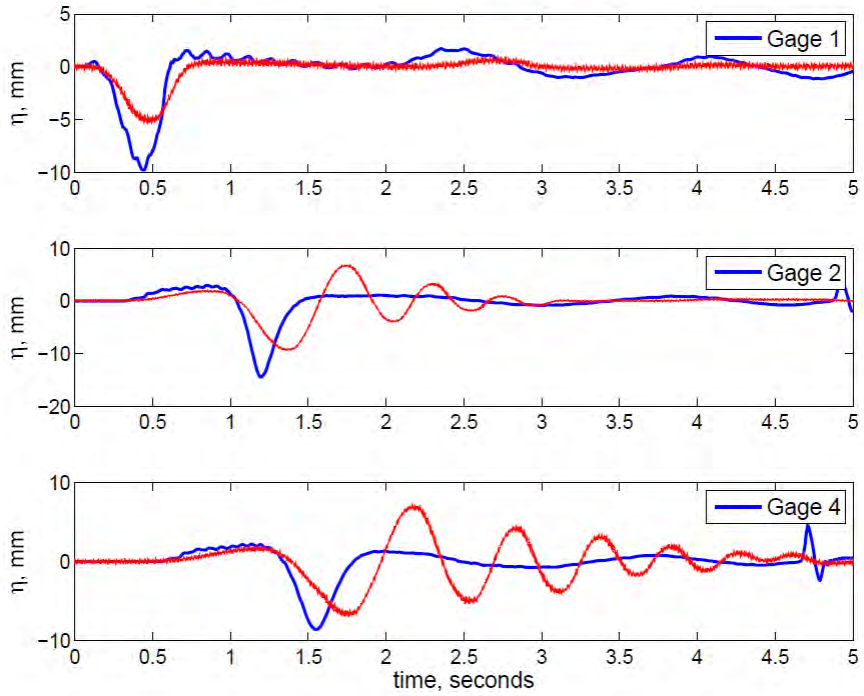

Figure 2b: Comparison of modeled (blue) and computed (red) water level dynamics for the initial submergence d=120 mm.

The presented modeling results overestimate the initial water withdraw at Gage 1 and miss a dispersive wave train generated at other gauges.

In addition to modeling water level at several gages, we recorded a time history of runup along the tank's center line. Figure 2 shows the runup for cases d=61 and 120 mm. According to the numerical results, the water first withdraws from the beach and then floods it. In the laboratory experiment, the runup values were measured using a small digital camera directly viewing the waterline motion over a graduated scale. The maximum measured runup values for d=61 and 120 mm are 6.2 and 3.4 mm, respectively. The modeling results (Figure 2) show a good comparison with the measured values and imply that the shallow water equations can capture the local runup at the slide.

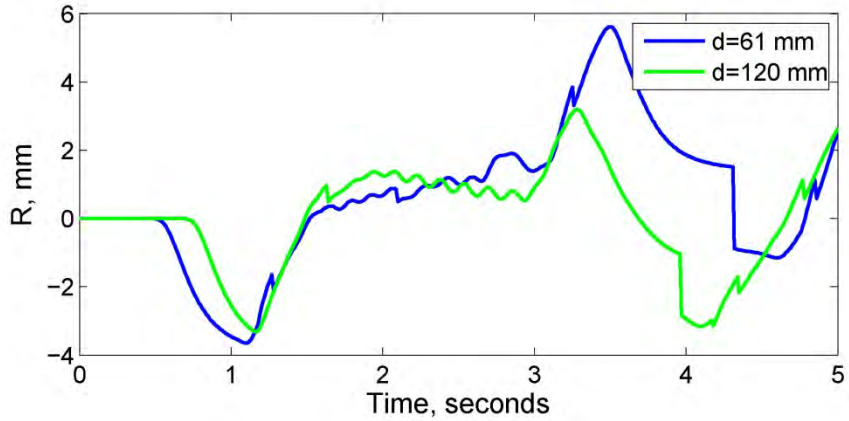

Figure 2: Modeled runup along the center line for the initial submergence d=61 and 120 mm.

Problem #4: Two-dimensional submarine granular slide

This benchmark problem is based on 2D laboratory experiments of Kimmoun and Dupont (2015; see Grilli *et al.,* 2016) in Ecole Centrale de Marseille's (IRPHE) precision tank (Marseille, France) (http://www1.udel.edu/kirby/landslide/problems/benchmark_4.html). During experiments, the deforming slide shape was recorded with a high-speed video camera. Similar to the previous benchmark problem, we set $\Delta x=0.005$ m and $\Delta t=1\cdot10^{-5}$ s.

First, we calibrate the viscous slide friction μ_s and obtain a good correlation with the observed slide at t=0.47s. The comparison of the modeled and measured water level dynamics is shown in Figure 3.

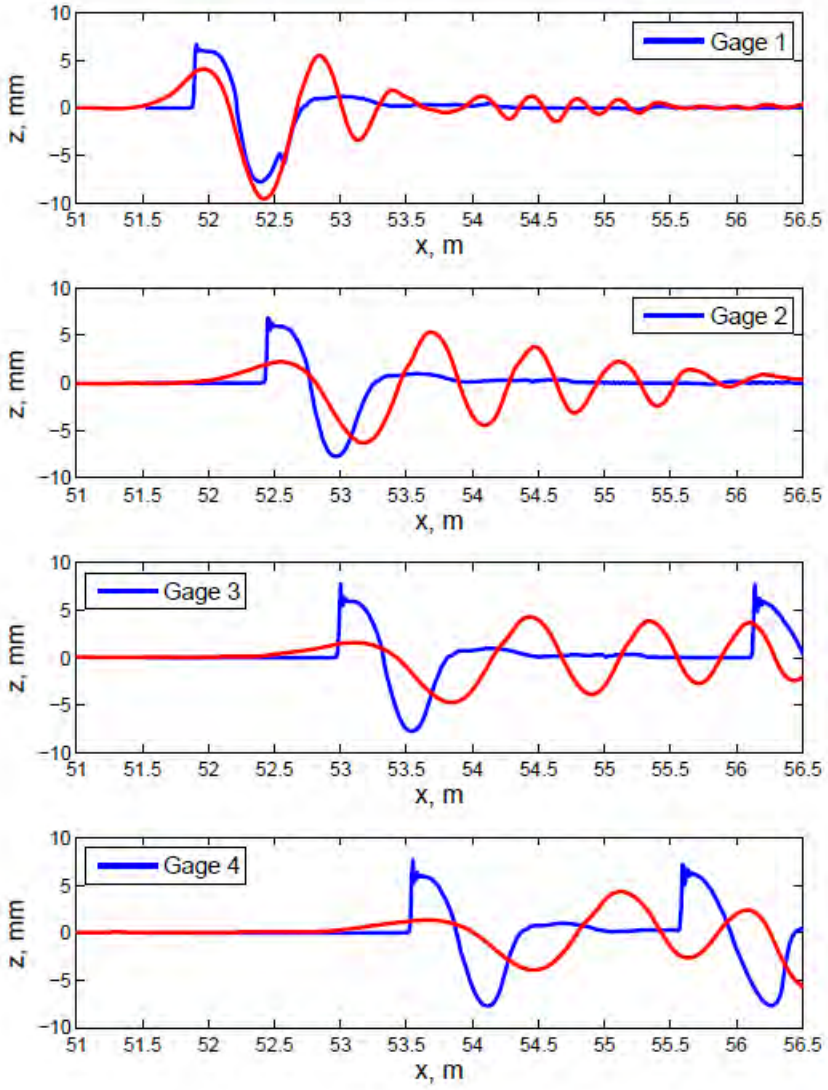

Figure 3: Comparison of modeled (blue) and computed (red) water level dynamics for test 17.

Similar to the benchmark problem 2, the shallow water equations have difficulties reproducing the dispersive wave train observed in the laboratory experiments. The maximum wave height at each gage is over estimated.

Problem #7: Slide at Port Valdez, AK

This benchmark problem is based on the historical event which occurred at Port Valdez, AK during the Alaska Earthquake of March 27, 1964. The event has previously been in recent studies by Parsons *et al.,* (2014) and Nicolsky *et al.,* (2013). The second document provides an overview of the historical background and geology for the site, and is the source for the problem described at http://www1.udel.edu/kirby/landslide/problems/benchmark_7.html.

We simulate waves generated by the HPV_{64} slide; the modeled inundation is shown in figure 4. The observed extent of the inundation after the 1964 earthquake is shown by the solid yellow line. Note that the 1964 tsunami inundated along the streets, but did not flood inside of the city blocks.

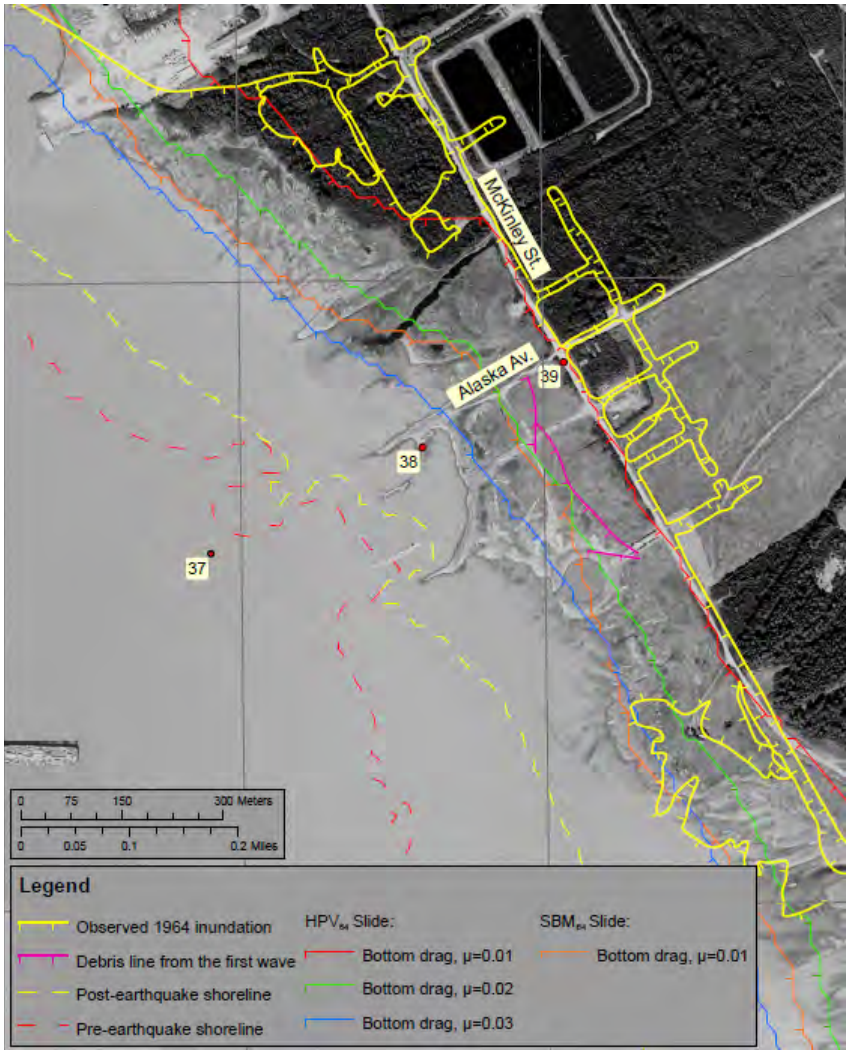

Figure 4: Sensitivity of inundation by the HPV64 slide-generated tsunami in the old townsite with respect to the parameterization of the bottom drag. The yellow line represents observed inundation in 1964 caused by both the landslide- and tectonically-generated tsunamis. The modeled MLLW shoreline before the earthquake is shown by a dashed yellow line. Hachures indicate the water side of the inundation lines.

The comparison of the modeled and observed extents of inundation is hindered by high snow berms in the town and deep consolidated snow cover at the time of the earthquake. The berms could have channeled the water and restricted its distribution (Coulter and Migliaccio, 1966). The dry 'islands' in the inundation zone are marked by the line with hachures pointing into the inundated area. The yellow line probably encompasses the composite inundation by both the landslide-generated and tectonic tsunamis.

The debris line from the first wave is shown in solid violet. We note that many buildings either collapsed or disintegrated when they were struck by the first wave, hence the debris could have been primarily composed of the coarse construction material, as shown in photographs in Wilson and Tørum (1968). We speculate that water carried by the first wave probably flooded beyond the debris line. The latter is confirmed by Coulter and Migliaccio (1966), who stated that the first wave reached McKinley Street, but did not flood beyond it except for a few locations. Thus, the debris line could not be directly used to calibrate the modeling results.

The modeling results presented in figure 4 reveal that the extent of the simulated tsunami inundation is sensitive to parameterization of the bottom drag coefficient, that is, the surface roughness coefficient μ in the Manning formula (Nicolsky and others, 2011a). The maximum modeled tsunami inundation for three values of the surface roughness, μ=0.01, 0.02 $m^{1/3}/s$ (0.015, 0.03 $ft^{1/3}/s$), and 0.03 $m^{1/3}/s$ (0.045 $ft^{1/3}/s$), are plotted by solid red, green, and blue lines, respectively. The best comparison with observations is obtained when the roughness μ is equal to 0.01 $m^{1/3}/s$ (0.015 $ft^{1/3}/s$), which corresponds to the roughness of smooth metal. A second good comparison is related to μ=0.02 $m^{1/3}/s$ (0.03 $ft^{1/3}/s$) that corresponds to firm gravel.

Time series of the modeled water wave height at three locations in the old city waterfront along Alaska Avenue are shown in figure 5.

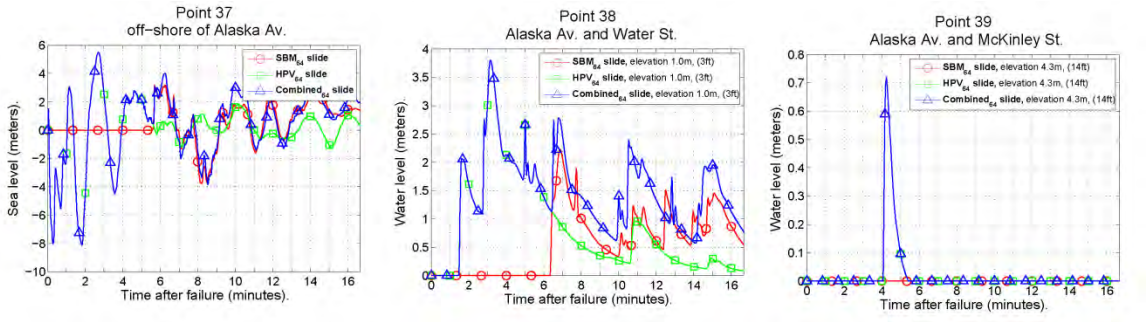

Figure 5: Modeled water level above ground at points 37, 38, and 39 along Alaska Avenue (figure 4 shows locations) during the 1964 tsunami.

4. Lessons learned

A numerical model used to simulate runup of landslide-generated tsunami is checked against the laboratory measurements and field observations. In computer experiments for BM2 and BM4, the shallow water equations showed difficulties in reproducing a dispersive wave train. However, despite of these limitations in BM2, the model reproduced the runup along the tank's center line. This implies that an extent of inundation at the slide origin is likely governed by the initial acceleration and other parameters; the wave dispersion is likely to be important when waves have enough time to propagate.

Modeling of the 1964 landslide at the head of Port Valdez shows that the extent of inundation depends on surface roughness and the initial slide volume.

5. References

Coulter, H.W., and Migliaccio, R.R., 1966, Effects of the earthquake of March 27, 1964 at Valdez, Alaska: U.S. Geological Survey Professional Paper, 542-C, 36 p.

Enet, F., Grilli, S.T., 2007. Experimental study of tsunami generation by three dimensional rigid underwater landslides. J. Waterway Port Coastal Ocean Eng. 133, 442–454.

Fine, I., Rabinovich, A., Kulikov, E., Thomson, R., and Bornhold, B., 1998, Numerical modeling of landslide-generated tsunamis with application to the Skagway Harbor tsunami of November 3, 1994, *in* Proceedings of international conference on tsunamis: Paris, p. 211–223.

Grilli S.T., Shelby M., Kimmoun O., Dupont G., Nicolsky D., Ma G., Kirby J.T. and Shi F., 2016, Modeling coastal tsunami hazard from submarine mass failures: effect of slide rheology, experimental validation, and case studies off the US East coast, *Natural Hazards*.

Jiang, L., and LeBlond, P., 1992, The coupling of a submarine slide and the surface waves which it generates: Journal of Geophysical Research, 97(C8):12,731–12,744.

Jiang, L., and LeBlond, P., 1994, Three-dimensional modeling of tsunami generation due to a submarine mudslide: Journal of Physical Oceanography, 24(3):559–572.

Kulikov, E.A., Rabinovich, A.B., Fine, I.V., Bornhold, B.D., and Thomson, R.E., 1998, Tsunami generation by landslides at the Pacific coast of North America and the role of tides: Oceanology, v. 38, no. 3, p. 323–328.

Ma G., Shi F. and Kirby J.T., 2012, Shock-capturing non-hydrostatic model for fully dispersive surface wave processes, *Ocean Modeling*, 43-44, 22-35

Nicolsky, D. J., Suleimani, E., and Hansen, R., 2011, Pure and Applied Geophysics, Validation and verification of a numerical model for tsunami propagation and runup, 168:1199–1222.

Nicolsky, D.J., Suleimani, E.N., Combellick, R.A., and Hansen, R.A., 2011b, Tsunami inundation maps of Whittier and western Passage Canal, Alaska: Alaska Division of Geological & Geophysical Surveys Report of Investigation 2011-7, 65 p.

Nicolsky, D.J., Suleimani, E.N., Haeussler, P.J., Ryan, H.F., Koehler, R.D., Combellick, R.A., and Hansen, R.A., 2013, Tsunami inundation maps of Port Valdez, Alaska: Alaska Division of Geological & Geophysical Surveys Report of Investigation 2013-1, 77 p.

Parsons, T., Geist, E.L., Ryan, H.F., Lee, H.J., Haeussler, P.J., Lynett, P., Hart, P.E., Sliter, R., Roland, E., 2014. Source and progression of a submarine landslide and tsunami: the 1964 Great Alaska earthquake at Valdez. J. Geophys. Res., Solid Earth119 (11), 8502–8516.

Suleimani, E., Nicolsky, D., Haeussler, P., and Hansen, R., 2011, Combined effects of tectonic and landslide-generated tsunami runup at Seward, Alaska during the M_w9.2 1964 earthquake, Pure Appl. Geophys 168, pp. 1053--1074.

Synolakis, C., and Bernard, E., 2006, Tsunami science before and beyond Boxing Day 2004:Philosophical Transactions of the Royal Society A, v. 364, n. 1845, p. 2231–2265.

Wilson, B.W., and Tørum, Alf, 1968, The tsunami of the Alaskan Earthquake, 1964—Engineering evaluation: Fort Belvoir, Virginia, U.S. Army Corps of Engineers Coastal Engineering Research Center, Technical Memorandum No. 25, 410 p.